Available online at www.sciencedirect.com
SCIENCE DIRECT®
Journal of Nuclear Materials 345 (2005) 65–74
journal of nuclear materials
www.elsevier.com/locate/jnucmat

Copper precipitate hardening of irradiated RPV materials and implications on the superposition law and re-irradiation kinetics

R. Chaouadi [a,*], R. Gérard [b]

[a] SCK·CEN, Boeretang 200, 2400 Mol, Belgium
[b] Tractebel Engineering, Avenue Ariane 7, 1200 Brussels, Belgium

Received 27 January 2005; accepted 6 May 2005

Abstract

Copper is known to play an important role in irradiation hardening and embrittlement of RPV materials. This is particularly true for old vessels. Indeed, while the Cu-content is low (<0.1%) in modern RPV materials, it often exceeded 0.15% in older vessels. Within the RADAMO irradiation program aiming to provide a reliable and extensive (chemistry, heat treatments, fluence, irradiation temperature) databank to investigate irradiation-induced hardening of RPV materials, we irradiated steels and welds with copper contents ranging from 0.06 to 0.31% at 300 and 265 °C. Experiments on re-irradiation after annealing were also performed to investigate the re-irradiation kinetics. It is found that copper plays a role in the very early stage of irradiation but saturates quite rapidly. The peak hardening is in agreement with the ageing data. Considering a two-component model, the linear superposition law provides the most appropriate one to rationalize the experimental data including re-irradiation path.

1. Introduction

There is a worldwide tendency in the international scientific community involved in irradiation effects on materials to promote physically-based rather than empirical or semi-empirical models. A large number of international groups in Europe, in Japan and in the US are putting their efforts together to provide tools able to predict materials behavior under specific irradiation conditions. Of course, the output of such research will be very much dependent on experimental data on which they rely. However, for historical reasons, most of the available experimental data that are used to qualify the various models are basically Charpy impact data. More specifically, the main parameter that is used to measure the degree of embrittlement is the ductile-to-brittle transition temperature (DBTT) which is not a fundamental material property. However, because of its small size and because a correlation between the DBTT-shift and the change of nil-ductility temperature (NDT) was established, which, in turn, is indexed to fracture toughness, the Charpy test was selected in surveillance programs to monitor the irradiation-induced degradation of the materials. Most of the R&D programs that have been implemented have used this test

* Corresponding author. Tel.: +32 14 33 21 90; fax: +32 14 32 15 29.
E-mail address: rchaouad@sckcen.be (R. Chaouadi).

0022-3115/$ - see front matter © 2005 Elsevier B.V. All rights reserved.
doi:10.1016/j.jnucmat.2005.05.001

as well. Nowadays, this test became the reference test in most of irradiation programs for characterizing a wide variety of materials although there are serious questions about its capability to accurately monitor irradiation damage. A minimum of eight Charpy impact specimens are usually needed to accurately define the transition temperature, the number of specimens depends on the scatter of the impact test data which in turn is related to material homogeneity. In the R&D programs supporting surveillance programs, because of the limited space available for irradiation and the inherent costs, not only irradiation but also testing costs, the number of irradiation conditions (fluence, flux, irradiation temperature) and materials (product form, chemistry, heat treatment) is often limited. Irradiation effects on the behavior of reactor pressure vessel (RPV) materials are also known to be sensitive to a large number of parameters, whether related to the material itself (chemical composition, microstructure) or to the irradiation conditions (irradiation temperature, neutron fluence, neutron flux). Because of the variety of the above mentioned parameters, it is therefore extremely difficult to find data where a full picture can be obtained.

The yield strength, on the other hand, provides a more appropriate parameter to investigate irradiation damage. Unfortunately, this test was not so popular in comparison to the Charpy impact test as it does not provide a direct link to fracture toughness. On the other hand, from the materials science point of view, the tensile test is the test that should be used. Indeed, fundamentally, it is known that irradiation produces nanosize defects that act as obstacles to dislocation motion. This translates into additional hardening and embrittlement of the material. The hardening can be determined by measuring the change of the yield strength (tensile testing) while embrittlement is determined by measuring the change of the DBTT (Charpy impact testing). In both cases, the involved mechanisms could be associated with the same physics, namely, dislocation motion in presence of obstacles. The latter has a theoretical framework with the known 'dispersion hardening barrier' model.

Therefore, an extensive experimental program, called RADAMO, was specifically oriented to the irradiation effects on the tensile properties of RPV materials [1]. Fourteen RPV materials were irradiated in the BR2 materials test reactor under well controlled conditions. The main objective of the RADAMO irradiation program is to provide a well documented and reliable databank on irradiation effects on the tensile properties of RPV materials to support the radiation damage modeling activities occurring at SCK·CEN. One advantage of such an experimental program is that all materials are irradiated and tested in similar conditions. It is known that alloying elements and impurities play an important role in the radiation susceptibility of RPV materials. Therefore, we selected a variety of RPV materials (plates, forgings and welds), with different chemical compositions (in particular their Cu, Ni and P content) irradiated at two irradiation temperatures (265 and 300 °C) to a neutron fluence ranging from low ($<1\times10^{19}$) to high ($>1\times10^{20}$ n/cm^2). Details on the irradiation, materials and test results can be found in [1].

The main objective of this paper is to investigate the copper content effect on the irradiation sensitivity of four selected RPV materials that differ mainly in their copper content. Nickel and phosphorus are essentially similar. It is known that copper is one of the key elements responsible for irradiation hardening and embrittlement of RPV materials. This is particularly true for old vessels where Cu, present as a residual element, was not well controlled. Indeed, while the Cu-content is low (<0.1%) in modern RPV materials, it was often exceeding 0.15% in older vessels.

2. Materials

We selected four RPV materials, 73W, 72W, 18MND5 and 16MND5 that exhibit significant changes in copper content while other elements, in particular those known for their irradiation sensitivity, remain essentially similar. Two additional materials, JRQ and A508 Weld, were selected to investigate the irradiation/annealing/re-irradiation (IAR) kinetics. The chemical composition and the heat treatment history of these materials are given in Tables 1 and 2, respectively. The tensile properties in the unirradiated condition are given in Table 3.

3. Irradiation conditions

The RADAMO irradiation program consisted of irradiating small tensile specimens of fourteen RPV materials in well controlled conditions placed into the

Table 1
Materials and heat treatments

Material	Type	Product form	Heat treatments
73W	SAW	Weld	SR 607 °C/40 h
72W	SAW	Weld	SR 607 °C/40 h
18MND5	A533B Cl.1	Plate	900 °C/WQ; 640 °C/5 h + 615 °C/15 h
16MND5	A508 Cl.3	Forging	910 °C WQ; 660 °C/4 h
JRQ	A533B	Plate	900 °C/WQ; 665 °C/12 h + 620 °C/40 h
A508	A508 Cl.3	Weld	SR 610 °C/5 h

SAW: submerged-arc welding; SR: stress relieve; WQ: water quench.

Table 2
Chemical composition (wt%)

Material	Cu	Ni	P	C	Si	Mn	S	Cr	Mo
73W	0.31	0.60	0.005	0.10	0.45	1.56	0.005	0.25	0.58
72W	0.23	0.60	0.006	0.09	0.44	1.60	0.006	0.27	0.58
18MND5	0.13	0.64	0.008	0.18	0.25	1.55	0.002	0.18	0.50
16MND5	0.06	0.69	0.013	0.14	0.04	1.37	0.009	0.13	0.52
JRQ	0.14	0.84	0.017	0.18	0.24	1.42	0.004	0.14	0.51
A508	0.07	0.83	0.015	0.07	0.15	1.15	0.005	0.14	0.55

Table 3
Tensile properties at 25 °C

Material	Yield strength σ_y (MPa)	Tensile strength σ_u (MPa)	Uniform elongation ε_u (%)	Total elongation ε_t (%)	Reduction of area RA (%)
73W	490	600	8	22	68
72W	498	606	8	20	67
18MND5	534	668	9	21	74
16MND5	488	616	10	24	70
JRQ	485	622	8	20	75
A508	545	637	8	19	76

Callisto loop of the BR2 materials test reactor. For each material and condition, 3–4 specimens were irradiated. These tensile specimens were loaded into small cylindrical capsules mounted in a rod that takes place into one of the in-pile sections of the Callisto loop. Each capsule contains 12–16 tensile specimens and 2 Fe-dosimeters located at both ends of the capsule. The neutron flux varies with the irradiation time and position into the reactor. For 73W, 18MND5 and 16MND5 irradiated at 300 °C, the neutron flux is close to 6×10^{13} n/cm^2 s while for 72W, the flux varies between 0.5 and 6×10^{13} n/cm^2 s. The neutron flux varies between 0.2 and 7.6×10^{13} n/cm^2 s for all materials irradiated at 265 °C as the irradiation time was constant and equal to 28 days. The specimens are in direct contact with the pressurized water. The dosimetry measurements were in agreement with the analytical calculations and, therefore, one can estimate the fluence at any other location. By this way, we can allocate a single neutron fluence/flux value to each specimen. The 16MND5 was not irradiated within the RADAMO program. It was selected because of its low copper content and its nickel content close to other materials. It was irradiated at 300 °C within the REVE project at SCK·CEN in the BR2 reactor [2].

Some of the materials, 73W, JRQ and A508 Weld were irradiated at 300 °C to a fluence of about 4×10^{19} n/cm^2, $E > 1$ MeV, and re-irradiated after an annealing heat treatment at 450 °C/150 h. The objective of this irradiation was to investigate the re-irradiation kinetics after annealing and therefore separate the various radiation damage mechanisms. More details will be given in the corresponding section.

4. Experimental results

The tensile specimens are 24 mm long, with a cylindrical gauge section of 2.4 mm diameter and 12 mm long. All tests were performed on an Instron 1341 machine in the hot cell, at room temperature under a constant crosshead speed of 0.1 mm/min, corresponding to a strain rate of 1.4×10^{-4} s^{-1}. We tested systematically two to four samples from each material and condition.

The test temperature, $\simeq$25 °C, was chosen because the irradiation-induced yield strength increase does not depend on test temperature [1]. Indeed, there is a unique temperature dependence of the yield strength for a large number of RPV materials, for static as well as dynamic loading [1]. This means that only the athermal part of the yield strength is affected by irradiation. Therefore, the irradiation-induced hardening can be evaluated at a single test temperature, room temperature being the most appropriate.

The increase of the yield strength as a function of fast (>1 MeV) neutron fluence of the four materials is shown in Figs. 1 and 2 for the 300 °C and 265 °C irradiation temperature, respectively. There is a clear copper effect on the magnitude of radiation-induced hardening of these materials. Moreover, within the neutron fluence window examined here, no saturation is reached.

First examination of the results shown in Figs. 1 and 2 supported by results on other materials [1] and literature, for example [3] and [4], indicate that:

1. The rate of copper precipitation is very fast in the early stage of irradiation and quite independent of copper content, only the strengthening magnitude

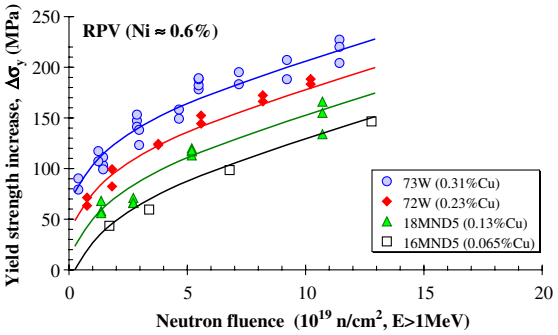

Fig. 1. Cu-content effect on the radiation hardening kinetics of RPV materials at T_{irrad} = 300 °C. The solid lines (trend curves) are identical, they differ only in their magnitude (obtained by a vertical translation).

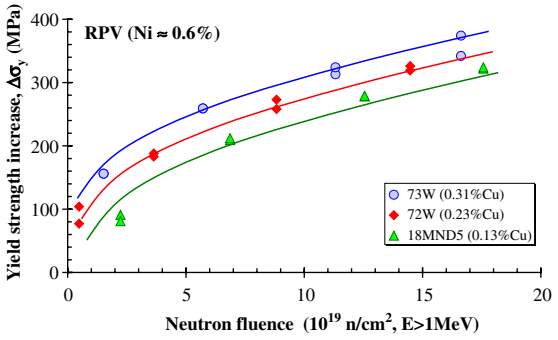

Fig. 2. Cu-content effect on the radiation hardening kinetics of RPV materials at T_{irrad} = 265 °C. The solid lines (trend curves) are identical, they differ only in their magnitude (obtained by a vertical translation).

increases with copper content. The maximum hardening due to copper precipitation seems to be reached after a neutron fluence of about $\simeq 1 \times 10^{19}$ n/cm^2, $E > 1$ MeV, in agreement with [5] (see high copper materials).

2. Above $\simeq 2 \times 10^{19}$ n/cm^2, the hardening rate becomes constant (about 10 MPa per 10^{19} n/cm^2) and independent of copper content.
3. Despite the limited data in the low fluence range of the specimens irradiated at 265 °C, there is a negligible effect of irradiation temperature on copper precipitation, in agreement with [5].
4. A direct consequence of these data, and it will be reinforced later, is that they suggest a linear superposition law of the contribution of copper-rich precipitates and matrix defects.

In the following, the copper contribution into hardening will be estimated based on a number of considerations that will be explicitly developed in the following section.

5. Radiation hardening mechanisms

Modeling irradiation-induced hardening of RPV materials has stimulated an important research within the scientific community. However, a model fully describing the underlying mechanisms has not been achieved yet. This is due to the difficulties associated with complex phenomena occurring in real materials. Nevertheless, some models are already available, with a limited application area, but that can reasonably describe a number of experimental data.

It is generally admitted that the total hardening is mainly the result of two distinct mechanisms, precipitation and matrix hardening, respectively [3,6–8]. The first mechanism is related to radiation-enhanced diffusion of some solute elements and their clustering. Copper and phosphorus have been identified for their sensitivity to form copper-rich precipitates (CRP) and phosphorus-rich precipitates (PRP) [9]. Under some circumstances, which are not met by our materials, manganese and nickel can form manganese–nickel-rich precipitates (MNP) [10,11]. In the present report with the materials under consideration, CRP is the dominant precipitation hardening mechanism.

The precipitation hardening can be explained by the excess defects introduced by irradiation that accelerate the diffusion of Cu. Copper has received a lot of attention because of its presence (0.1–0.3%) in a number of earlier RPV materials. This mechanism is reasonably well understood and has benefited from support of microstructural observations.

The second mechanism, usually referred to as matrix damage, is not fully understood. Basically, this second mechanism consists of point defect clusters, mainly vacancy-solute complexes. Unfortunately, available microstructural techniques are not yet able to fully characterize them despite large efforts devoted to determine their size and nature with advanced techniques (APFIM, SANS, PAS) [12]. Nevertheless, dedicated experiments have allowed identifying a number of important features that can be used in modeling.

In the following, the knowledge of the detailed underlying mechanisms and their modeling are not necessary to reach the conclusions of the present paper. Only their identification is required together with some background information on their kinetics. It should be recalled that, as already mentioned, detailed modeling of irradiation-induced hardening is out of the scope of the present paper. The objective of this paper is to quantify the peak hardening due to copper precipitation and, as it will be seen, this is not much dependent on the details of the model but it has important implications on the structure of the model.

The irradiation-induced defects act as obstacles impeding dislocation motion. We can distinguish mainly two types of defects, the copper-rich precipitates

(CRP) and point defect (vacancy, interstitial) clusters that are usually referred to as matrix defects (MD). Most of available models are based on this assumption. The total observed hardening of the material is the result of the interaction of dislocation with these defects. The superposition law of these two defect contributions is an important issue. In practice, it is often taken as linear or quadratic although the actual superposition law depends on the strength of the obstacles [2,13–16]. In the linear superposition, it is implicitly assumed that there is no interaction between the mechanisms contrary to the quadratic one where such interaction exists. Between these two cases, an intermediate situation was proposed by Odette and Lucas [16] by introducing a superposition parameter, S, that was found to fit better the experimental data. However, this parameter depends on the strength of the defects (obstacles) which are a priori unknown. Therefore, in the following, we will consider this intermediate superposition law only if none of the linear and quadratic superposition seems to apply to rationalize the experimental data.

The total yield increase can be written as

$$\Delta\sigma^{p}_{\text{total}} = \Delta\sigma^{p}_{\text{CRP}} + \Delta\sigma^{p}_{\text{MD}}, \tag{1}$$

where $p = 1$ for the linear superposition and $p = 2$ for the quadratic one.

The total yield strength increase of our materials is known (experimentally measured), but the CRP and MD components are not. However, because these materials differ mainly in their copper content, it is reasonable to expect that the MD component should be similar for these materials. It is also known that the precipitation rate with neutron exposure is quite high, most of CRPs are formed at around 1×10^{19} n/cm^2, $E > 1$ MeV [1,3–5]. By examining the experimental data shown in Figs. 1 and 2, we can easily see that, by drawing a curve fitting the data of one material, the trend curves of other materials can be derived by a simple vertical translation of this fitting curve. This is illustrated in Figs. 1 and 2 where the solid lines are trend curves drawn to fit the experimental data. However, the shape of the curve was kept invariably, only the magnitude is changed through a vertical translation. There is a clear copper effect on the magnitude of the radiation-induced hardening of these materials. Above about 1×10^{19} n/cm^2, $E > 1$ MeV, the hardening kinetics is independent of the copper content. Because the shape of the trend curve remains essentially invariable with copper change, matrix damage being unaffected by copper, only a linear superposition (or close to linear) can lead to such a behavior. This supports a linear rather than a quadratic superposition of the CRP and MD radiation damage components. Additional support will be given later on the adequacy of the linear superposition rule in comparison the quadratic one.

In the following, the CRP component will be experimentally derived from the results of Figs. 1 and 2 assuming a linear superposition.

6. Copper hardening

The contribution of the CRP component is based on ageing studies of copper precipitation in ferrite, modified for irradiation to take into account the rate enhancement of copper atom diffusion, namely the Fisher et al. model [6,7,17]. The time to reach peak hardening is taken proportional to the vacancy concentration induced by irradiation. As a result, the time to peak is reduced by irradiation according to

$$t^{\text{irrad}}_{\text{peak}} = t^{\text{th}}_{\text{peak}} \frac{C^{\text{th}}_{\text{v}}}{C^{\text{irrad}}_{\text{v}}}, \tag{2}$$

where t_{peak} is the time to peak hardening, C_{v} is the vacancy concentration, the superscripts 'th' and 'irrad' refer, respectively, to thermal and irradiated.

Referring to the Fisher et al. model [6], the contribution to the yield strength increase of the CRPs can be written as

$$\Delta\sigma_{\text{CRP}} = f\left(\frac{C^{\text{th}}_{\text{v}}}{C^{\text{irrad}}_{\text{v}}}\right)\Delta\sigma^{\max}_{\text{CRP}}, \tag{3}$$

where $f\left(\frac{C^{\text{th}}_{\text{v}}}{C^{\text{irrad}}_{\text{v}}}\right)$ is a function describing the radiation-enhanced diffusion for copper precipitation, C_{v} is the vacancy concentration and $\Delta\sigma^{\max}_{\text{CRP}}$ is the maximum CRP hardening.

Based on thermal ageing experiments performed on Fe–Cu binary alloys, a linear relationship was found between the yield strength increase and the square root of the copper content [6,18]. However, the copper content in these alloys (0.6–6%) was much higher than actually found in RPV materials. No experimental data were available in the range of RPV interest. In the following, we will provide experimental data that can be compared to the curve established for ageing data.

Re-examining the experimental data and trend curves of Figs. 1 and 2, we determined the fluence independent additional hardening directly correlated to the copper content. The results are shown in Table 4 where the trend curve of 16MND5 is taken as a reference for the 300 °C irradiation and 18MND5 as a reference for the 265 °C irradiation data. The data were simultaneously fitted with an equation using a minimum number of parameters and keeping the shape of the curve unchanged. This way, the various curves differ only in the magnitude term resulting in vertically-shifted curves, each corresponding to a specific Cu-content. Taking one of the curves as reference, the difference with respect to reference is easily determined. The results are given in Table 4. The values represent the additional hardening

Table 4
Relative hardening of the various materials[a]

	T_{irrad}	
	300 °C	265 °C
73W	82	66
72W	57	36
18MND5	25	Reference
16MND5	Reference	n.a.

[a] Values are adjusted to the reference levels of 16MND5 for T_{irrad} = 300 °C and 18MND5 for T_{irrad} = 265 °C.

Table 5
Irradiation-induced peak hardening due to Cu-precipitation (absolute values)

	T_{irrad}	
	300 °C	265 °C
73W	107	116
72W	82	86
18MND5	50	50
16MND5	25	n.a.

with respect to the reference materials. The copper contributions for the reference materials, the 16MND5 and 18MND5 for the 300 and 265 °C irradiation, respectively, were estimated from the data in the low fluence range ($<1\times10^{19}$ n/cm^2, $E>1$ MeV), and supported by other experimental data where the copper content is similar. As a result, the copper contribution was estimated to be 25 and 50 MPa for 16MND5 and 18MND5, respectively. Replacing these reference values in Table 4, the actual copper contribution for each of the materials and irradiation temperature considered here were determined and reported in Table 5. Note that alternative methods of derivation of the copper contribution to hardening lead to comparable results. As it can be seen and in agreement with the available models, within the temperature range considered here, the irradiation temperature does not affect the copper precipitate component to hardening [4,5]. If CRP hardening is subtracted from the total hardening, we obtain Fig. 3 which is another indication of the consistency of the results, namely, there is a unique trend curve for matrix damage, independent of copper content.

It was already mentioned that based on the thermal ageing data, a linear relationship was found between yield strength increase and the square root of copper content. The data from Table 5 were added to the thermal ageing data used to establish the square root relation to copper content and are shown in Fig. 4. Two additional data points obtained on Fe–Cu binary alloys were also added. The irradiated data fall within the extrapolation of the Russell and Brown linear fitting curve [18] to the lower copper content. This is clearly

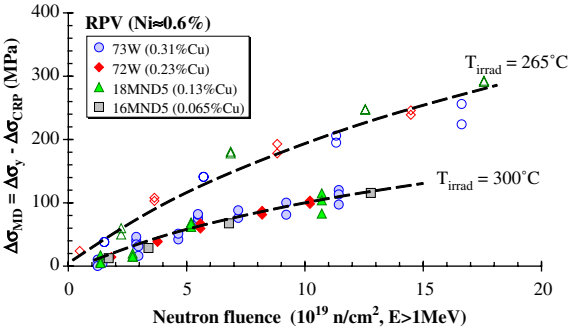

Fig. 3. Matrix hardening after subtracting the peak hardening contribution. All four materials fall within a single trend curve for both irradiation temperatures.

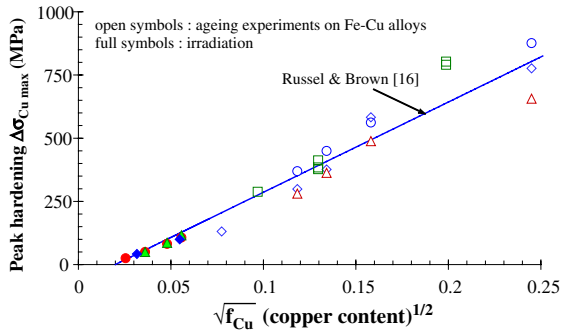

Fig. 4. Peak hardening versus copper content, thermal ageing versus irradiation.

supporting the concept of enhanced diffusion process as proposed by Fisher et al. [6] for the CRP mechanism.

Fig. 5 was obtained by considering the copper content range of interest for RPV materials. We have added some data taken from Lucas et al. [18] at a neutron fluence of 0.9×10^{19} n/cm^2, $E>1$ MeV, with Ni and P contents of about 0.8% and 0.005%, respectively. However, The best fit is obtained using the following equation:

$$\Delta\sigma_{CRP}^{max} = 215[1-\exp\{-2.7(\%Cu-0.03)\}]. \quad (4)$$

This relation can thus be used to estimate the maximum contribution of the CRP-component. Note that contrary to ageing experiments, no overageing is assumed to take place after peak hardening is reached [4,7]. The peak hardening relation, Eq. (4), compared to other analytical equations [19–21], was found in better agreement with the experimental data. Note that the above relation provides a saturation value above which the copper effect does not change. This is in agreement with FEGSTEM data of Williams and Ellis [22] which showed that matrix copper reaches a plateau value around 0.35% irrespective to the total bulk copper (up to 0.6%).

It is important to mention here that the matrix copper, i.e., the copper present in solution and that

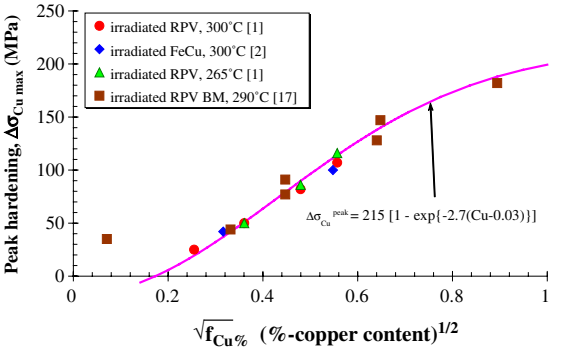

Fig. 5. Peak hardening versus copper content.

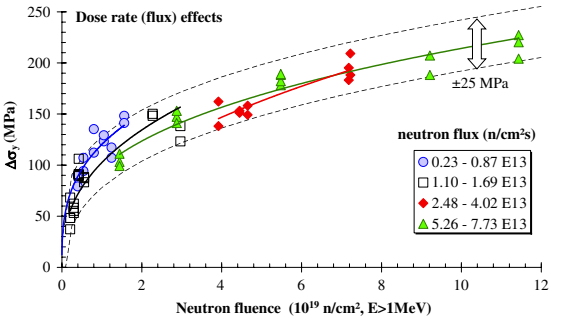

Fig. 7. Dose rate effects on the irradiation hardening of 73W. The small dose rate effect is within the experimental uncertainties.

can potentially precipitate, may be different from the bulk one. However, it is believed that in our materials, the matrix copper can be considered as very close to the bulk copper or, in other words, almost all copper is in solid solution. This is supported by our experimental data on a large number of materials. For the 73W weld, Miller et al. [23,24] reported a matrix copper as low as 0.12%. This value cannot be explained on the experimental testing basis. Nevertheless, in case the matrix copper values are available, the peak hardening equation (4) shown in Fig. 5 should be appropriately adapted.

7. Dose rate effects

The dose rate or flux effect is an important issue to understand the differences between surveillance and material test reactor data. One of the RPV materials irradiated in RADAMO, namely the 73W, offers the opportunity to investigate the dose rate effects within the range 2×10^{12} to 7×10^{13} n/cm^{2}s, $E>1$ MeV. In Fig. 6, we plotted the data obtained on 73W indicating the fluence and dose rate (flux) at each data point. It is hard to clearly distinguish any effect of dose rate. If the trend curves are included for each of the data sets

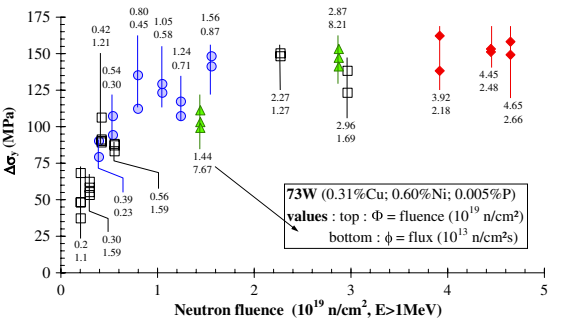

Fig. 6. Dose rate effects on the irradiation hardening of 73W.

as shown in Fig. 7, a small flux effect could be detected but this is within the experimental uncertainties. Therefore, we can consider that dose rate effects, at this stage, can be neglected. Of course, the experimental data we have here do not allow to provide a general rule, this would require a much larger databank (materials and irradiation conditions) including surveillance data. For the latter, the dose rate is much lower, in the range of 10^{11} n/cm^{2}s, $E>1$ MeV. The dose rate effect was considered to drastically affect the precipitate hardening above a certain fluence threshold [21,25]. The experimental data we have on 73W are not in agreement with this statement.

8. Matrix hardening

At this stage, it is possible to determine the maximum contribution of the CRP component into the total hardening. We know that this process is quite rapid and reaches its maximum value around a neutron fluence of about 1×10^{19} n/cm^2, $E>1$ MeV. Therefore, above certain neutron fluence when copper precipitation is achieved, the dominant mechanism is matrix damage. However, to be able to determine the matrix damage contribution, it is necessary to know how it combines with the precipitation damage component. More specifically, both precipitate and matrix damage contributions can be additive (linear sum) or interdependent. Therefore, the matrix damage contribution will depend on the superposition rule.

To illustrate this, the experimental data of Figs. 1 and 2 were used to determine the total hardening at three arbitrary selected fluence levels, namely, 2.5, 7.5 and 12.5×10^{19} n/cm^2, $E>1$ MeV. The CRP component is calculated using the analytical equation given in the previous section. By assuming either a linear or quadratic superposition law, we can derive the matrix damage component. The results are given in Tables 6 and 7, for 300 and 265 °C irradiation, respectively. The matrix

Table 6
Determination of matrix damage at T_{irrad} = 300 °C

Fluence	$>1\times10^{19}$ n/cm^2	2.5×10^{19} n/cm^2			7.5×10^{19} n/cm^2			12.5×10^{19} n/cm^2		
	$\Delta\sigma_{CRP}$	$\Delta\sigma_{total}$	$\Delta\sigma_{MD1}$	$\Delta\sigma_{MD2}$	$\Delta\sigma_{total}$	$\Delta\sigma_{MD1}$	$\Delta\sigma_{MD2}$	$\Delta\sigma_{total}$	$\Delta\sigma_{MD1}$	$\Delta\sigma_{MD2}$
73W	114	136	22	74	189	75	151	220	106	189
72W	90	106	16	56	164	74	137	201	111	180
18MND5	51	75	25	56	126	75	115	160	109	152
16MND5	19	53	33	49	104	84	102	142	123	141
$\Delta\sigma_{MD\ average}$			24 ± 7	59 ± 11		77 ± 5	126 ± 22		112 ± 7	165 ± 23

$\Delta\sigma_{MD1}$: matrix contribution assuming a linear superposition: $\Delta\sigma_{total} = \Delta\sigma_{CRP} + \Delta\sigma_{MD1}$.
$\Delta\sigma_{MD2}$: matrix contribution assuming a quadratic superposition: $\Delta\sigma^2_{total} = \Delta\sigma^2_{CRP} + \Delta\sigma^2_{MD\ 2}$.

Table 7
Determination of matrix damage at T_{irrad} = 265 °C

Fluence	$>1\times10^{19}$ n/cm^2	2.5×10^{19} n/cm^2			7.5×10^{19} n/cm^2			12.5×10^{19} n/cm^2		
	$\Delta\sigma_{CRP}$	$\Delta\sigma_{total}$	$\Delta\sigma_{MD1}$	$\Delta\sigma_{MD2}$	$\Delta\sigma_{total}$	$\Delta\sigma_{MD1}$	$\Delta\sigma_{MD2}$	$\Delta\sigma_{total}$	$\Delta\sigma_{MD1}$	$\Delta\sigma_{MD2}$
73W	114	188	74	150	276	162	251	330	216	309
72W	90	165	75	138	249	159	232	302	212	288
18MND5	51	108	57	95	197	146	190	261	210	256
$\Delta\sigma_{MD\ average}$			69 ± 10	128 ± 29		156 ± 8	225 ± 31		212 ± 3	284 ± 27

$\Delta\sigma_{MD1}$: matrix contribution assuming a linear superposition: $\Delta\sigma_{total} = \Delta\sigma_{CRP} + \Delta\sigma_{MD1}$.
$\Delta\sigma_{MD2}$: matrix contribution assuming a quadratic superposition: $\Delta\sigma^2_{total} = \Delta\sigma^2_{CRP} + \Delta\sigma^2_{MD2}$.

damage is indicated by $\Delta\sigma_{MD1}$ for the linear superposition and $\Delta\sigma_{MD2}$ for the quadratic superposition. It should be recalled that all these materials differ mainly in their copper content, the other elements are very similar. Examination of Tables 6 and 7 clearly indicate that the linear superposition leads to a quasi material independent matrix damage value with the smallest standard deviation.

9. Mechanisms separation by irradiation/annealing/re-irradiation

Another experimental procedure to better select the appropriate superposition law is obtained by performing a dedicated experiment to separate the CRP and MD components. To determine the matrix damage contribution, we used the irradiation/annealing/re-irradiation data obtained on 73W, JRQ and A508 Weld. Indeed, after irradiation at 300 °C to 4.1×10^{19} n/cm^2, the specimens were annealed (450 °C/150 h) and further re-irradiated up to three levels of neutron fluence. The above thermal cycle was chosen after showing that it was successful in a full recovery of the initial tensile properties of a number of RPV materials [1]. This heat treatment was also found to produce a close to 100% recovery of the DBTT [26]. However, for the three materials under consideration, a small positive or negative residual stress with respect to the initial yield strength remains after annealing. This is taken into account for the re-irradiation path. At 4.1×10^{19} n/cm^2, it is considered that most of the copper available into solid solution has precipitated. After annealing at 450 °C for 150 h, the copper remaining into solution will decrease because of precipitate coarsening by the Ostwald ripening mechanism. The rate of further re-irradiation will consequently be reduced and the matrix damage can be estimated from this re-irradiation data. The results are shown in Figs. 8–10 which compare the irradiation to the re-irradiation path after annealing for the three materials. It should be noticed that not all the copper that

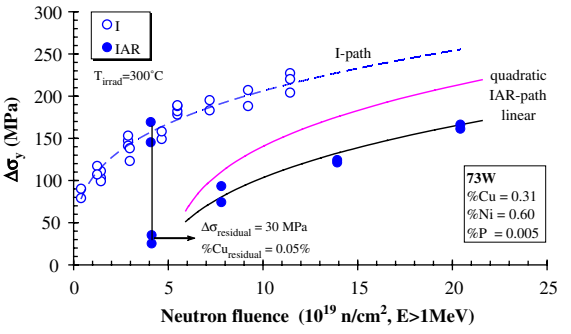

Fig. 8. Irradiation versus irradiation/annealing/re-irradiation (IAR) kinetics of 73W. The strengthening rate of the IAR path is significantly lower than the I-path as a result of Cu-precipitates coarsening.

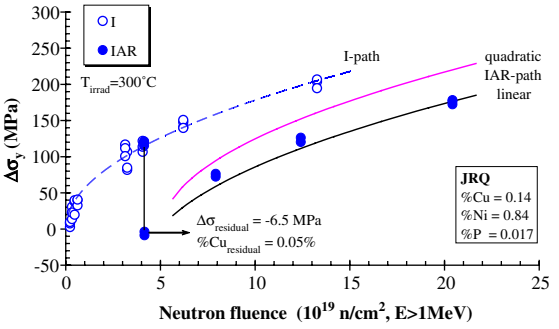

Fig. 9. Irradiation versus irradiation/annealing/re-irradiation (IAR) kinetics of JRQ. The strengthening rate of the IAR path is lower than the I-path as a result of Cu-precipitates coarsening.

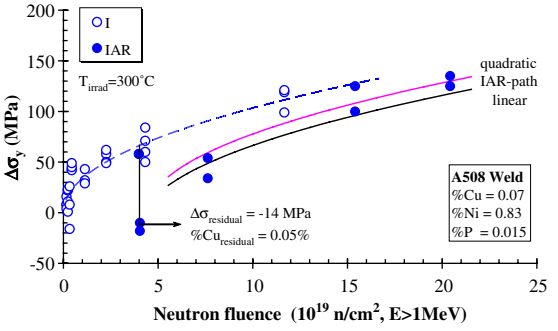

Fig. 10. Irradiation versus irradiation/annealing/re-irradiation (IAR) kinetics of A508 Weld. The strengthening rate of the IAR path is similar to the I-path.

precipitated will coarsen and would not be anymore available for further precipitation but a small amount usually remains into solution, probably around 0.05%. Therefore, in the re-irradiation path, we will consider that the annealed material has 0.05%Cu. This value is in agreement with the copper remaining in the matrix after irradiation as measured by Miller et al. [27]. We can derive the re-irradiation path simply by assuming a new material that has 0.05%Cu but using the same matrix damage kinetics as in the irradiation path. The solid curve for re-irradiation, obtained by considering a material with similar composition except for copper (0.05%), is in very good agreement with the experimental data of the three materials. This clearly supports the linear superposition law to be adequate to represent irradiation hardening of RPV steels. A quadratic superposition rule would have resulted in a higher hardening rate.

It is interesting to note that the results shown in Fig. 8 are in full agreement with the data of Sokolov et al. [28]. Indeed, the re-irradiation embrittlement becomes equal for HSST-02 plate (0.14% Cu) and 73W (0.31% Cu) and at a rate lower than for the irradiation path.

It is clearly demonstrated using two different experimental techniques, namely irradiation path of four materials with similar composition except copper content and re-irradiation kinetics of three materials with different chemical compositions, the linear superposition including precipitate and matrix hardening components is the most adequate. Nevertheless, other superposition laws are not excluded if other combinations of damage mechanisms are considered.

10. Conclusions

The irradiation effect on copper precipitation was experimentally evaluated by selecting a number of materials where copper is the major variable (0.06–0.31% Cu) while the other elements are essentially similar (≃0.6% Ni). We assumed a two-component damage mechanism, namely precipitate hardening and matrix hardening. The irradiation-induced precipitates are essentially copper-rich precipitates. The precipitate hardening reaches its saturation value, corresponding to peak hardening, already around 1×10^{19} n/cm^2, $E > 1$ MeV while matrix hardening increases continuously with neutron exposure. The experimental data allowed one to derive the peak hardening resulting from the copper-rich precipitates as matrix damage is basically similar for all the materials under consideration. It is found that the re-irradiation kinetics after annealing depends strongly on the material under consideration. Moreover, re-irradiation after annealing experiments were also used to question the relationship between the precipitate and matrix hardening components.

Two important conclusions can be drawn from the experimental work analyzed in this paper.

1. The basic idea of using the thermal ageing process to describe the irradiation-induced precipitate process is adequate. In particular, the peak hardening values as derived from thermal ageing and irradiation were found to fall within a unique curve proportional to the square root of copper content.
2. The adequate rule of superposition for the copper-rich precipitate and matrix damage components is the linear one. The experimental data including the re-irradiation results could be rationalized using this rule.

However, because of the lack of microstructural characterization, the matrix copper (present into solution) was assumed to be equal to the bulk copper. This assumption is believed to be not wrong as it was possible to rationalize the various experimental data using this assumption. However, in a number of cases when experimental data are available from literature, a good agreement was found. Therefore, it is believed that the bulk composition is close to the matrix composition.

It is important to mention that the possibility of another superposition law, quadratic for instance, cannot be excluded if alternative models including other damage mechanisms are considered. However, the experimental data presented here suggest a linear superposition of the two-component model.

Acknowledgement

This work was performed within the convention 'Electrabel – SCK·CEN' 2003 under the task damage modeling and micromechanics. The authors gratefully acknowledge the LHMA staff for the experimental work performed in the hot cells, in particular P. Wouters for his professional quality. Our sincere thanks are to R. Nanstad for providing the 72W and 73W weld metals. Finally, special gratitude goes to A. Fabry whose ideas have greatly influenced the present work.

References

[1] R. Chaouadi, RADAMO – an experimental databank for investigating irradiation strengthening of RPV materials, Report SCK·CEN R-3858, 2004.
[2] L. Malerba, Multiscale modeling and modeling oriented experiments at SCK·CEN, Report SCK·CEN R-3709, 2003.
[3] G.E. Lucas, G.R. Odette, P.M. Lombrozo, J.W. Scheckherd, in: F.A. Garner et al. (Eds.), Effects of Radiation on Materials: 12th International Symposium, ASTM STP, vol. 870, ASTM, 1985, p. 900.
[4] T.J. Williams, P.R. Burch, C.A. English, P.H.N. de la cour Ray, in: G.J. Theus, J.R. Weeks (Eds.), Proceedings of the 3rd International Symposium on Environmental Degradation of Materials in Nuclear Power Systems – Water Reactors, 1988, p. 121.
[5] B.D. Wirth, G.R. Odette, W.R. Pavinich, G.E. Lucas, S.E. Spooner, in: R.K. Nanstad et al. (Eds.), Effects of Radiation on Materials: 18th International Symposium, ASTM STP, vol. 1325, ASTM, 1999, p. 102.
[6] S.B. Fisher, J.E. Harbottle, N. Aldridge, Philos. Trans. Roy. Soc. London A 315 (1985) 301.
[7] J.T. Buswell, R.B. Jones, in: A.S. Kumar et al. (Eds.), Effects of Radiation on Materials: 16th International Symposium, ASTM STP, vol. 1175, ASTM, 1993, p. 424.
[8] E.D. Eason, J.E. Wright, R.G. Odette, Improved embrittlement correlations for reactor pressure vessel steels, Report NUREG/CR-6551, 1998.
[9] M.M. Ghoniem, F.H. Hammad, Int. J. Press. Vess. Piping 74 (1997) 189.
[10] R.G. Odette, Radiation induced microstructural evolution in reactor pressure vessel steels, MRS Symp. Proc. 373 (1995) 137.
[11] G.R. Odette, B.D. Wirth, in: S. Ishino et al. (Eds.), Proceedings of the International Symposium on Mechanisms of Material Degradation and Non-Destructive Evaluation in Light Water Reactors, 2002, p. 77.
[12] C.A. English, J.M. Hyde, S.R. Ortner, in: S. Ishino et al. (Eds.), Proceedings of the International Symposium on Mechanisms of Material Degradation and Non-Destructive Evaluation in Light Water Reactors, 2002, p. 53.
[13] A.J.E. Foreman, M.J. Makin, Can. J. Phys. 45 (1967) 511.
[14] L.M. Brown, R.K. Ham, in: A. Kelly, R.B. Nicholson (Eds.), Strengthening Methods in Crystals, Applied Science Publishers, 1971, p. 9.
[15] U.F. Kocks, A.S. Argon, M.F. Ashby, Prog. Mater. Sci. 19 (1975).
[16] G.R. Odette, G.E. Lucas, Radiat. Eff. Def. Solids 144 (1998) 189.
[17] R. Chaouadi, Status report on radiation damage modeling of reactor pressure vessel steels, Report SCK·CEN R-3538, 2001.
[18] K.C. Russell, L.M. Brown, Acta Metall. 20 (1972) 969.
[19] G.E. Lucas, G.R. Odette, R. Maiti, J.W. Sheckherd, in: F.A. Garner et al. (Eds.), Influence of Radiation on Material Properties: 13th International Symposium (Part II), ASTM STP, vol. 956, ASTM, 1987, p. 379.
[20] G.R. Odette, G.E. Lucas, in: L.E. Steele (Ed.), Radiation Embrittlement of Nuclear Reactor Pressure Vessel Steels: An International Review (Second Volume), ASTM STP, vol. 909, ASTM, 1986, p. 202.
[21] A. Fabry, J. Van de Velde, J.L. Puzzolante, T. Van Ransbeeck, A. Verstrepen, E.C. Biemiller, R.G. Carter, T. Petrova, in: D.S. Gelles et al. (Eds.), Effects of Irradiation on Materials: 17th International Symposium, ASTM STP, vol. 1270, ASTM, 1996, p. 138.
[22] T.J. Williams, D. Ellis, in: S.T. Rosinski et al. (Eds.), Effects of Radiation on Materials: 20th International Symposium, ASTM STP, vol. 1405, ASTM, 2001, p. 8.
[23] M.K. Miller, K.F. Russell, R.E. Stoller, P. Pareige, Atom probe tomography characterization of the solute distributions in a neutron-irradiated and annealed pressure vessel steel weld, NUREG/CR-6629, 2000.
[24] M.K. Miller, K.F. Russell, P. Pareige, Effect of annealing and re-irradiation on the copper-enriched precipitates in a neutron-irradiated pressure vessel steel weld, MRS Symp. Proc. 650 (2001) R3.15.1.
[25] G.R. Odette, G.E. Lucas, D. Klingensmith, in: R.K. Nanstad et al. (Eds.), Effects of Radiation on Materials: 18th International Symposium, ASTM STP, vol. 1325, ASTM, 1999, p. 88.
[26] S.K. Iskander, M.A. Sokolov, R.K. Nanstad, in: D.S. Gelles et al. (Eds.), Effects of Radiation on Materials: 17th International Symposium, ASTM STP, vol. 1270, ASTM, 277, 1996.
[27] M.K. Miller, P. Pareige, M.G. Burke, Mater. Charact. 44 (2000) 235.
[28] M.A. Sokolov, A.A. Chernobaeva, R.K. Nanstad, Y.A. Nikolaev, Y.N. Korolev, in: M.L. Hamilton et al. (Eds.), Effects of Irradiation on Materials: 19th International Symposium, ASTM STP, vol. 1366, ASTM, 2000, p. 415.